J Mater Sci (2006) 41:5455–5461
DOI 10.1007/s10853-006-0295-1

Study of γ_2 precipitation in Cu–Al–Be shape memory alloys

M. T. Ochoa-Lara · H. Flores-Zúñiga · D. Rios-Jara

Received: 21 July 2005 / Accepted: 18 October 2005 / Published online: 13 June 2006

Abstract Thermal aging between 250 and 500 °C of ordered β phase in a polycrystalline Cu–Al–Be shape memory alloy were performed, and the formation of phase γ_2 was studied with optical and transmission electron microscopies and XRD techniques. The growth of γ_2 phase shows a polynomial behavior, and Avrami curves as well as a Time–Temperature–Transformation diagram were constructed from these results. In addition, the formation of stable γ_2 precipitates was studied in aged Cu–Al–Be ribbons. The presence of α regions surrounding γ_2 precipitates for longer aging times at higher temperatures was observed, giving a consistent precipitation scheme.

Introduction

Copper based shape memory alloys have been used on a commercial basis for some years on account of their interesting thermomechanical properties, which include the shape memory effect, pseudoelasticity and high damping capacity. A martensitic phase transformation from a metastable β_1 phase, obtained at room temperature by quenching from its high temperature stability region (typically above 650 °C), to a metastable martensitic phase, is the origin of all those properties. In particular, Cu–Al–Be alloys show a good behavior at moderated temperatures (< 200 °C) because of the good thermal stability of the metastable β_1 phase [1]. This characteristic allows its use under conditions where other alloys fail because of the growing of stable α and γ_2 phases at these temperatures, which cancels the possibility for obtaining the desired effects. Indeed, the addition of small amounts of Beryllium to the Cu–Al alloy leads to an important decrease in the martensitic transformation temperature (M_S), without modifying the martensitic transformation nature [2]. Therefore, the alloy exhibits a unique adaptability for its use in high as well as low temperature actuator applications [3].

On the other hand, it is well known that introducing γ_2 phase precipitates into the matrix improves the strengthening of copper based shape memory alloys [4], but after some extent cause changes in M_S and the hysteresis of transformation, as was shown in other similar materials like Cu–Zn–Al [4–7].

The γ_2 (Al–Cu) is an equilibrium phase with a complex structure; this structure can be visualized as a cubic cell formed by $3 \times 3 \times 3$ ordered B2 type cubes (Fig. 1), where the atoms at the corners and at the center have been removed; which leads to shifts (not shown in Fig. 1) of the neighboring atoms to compensate the vacancies. Similarly, ordered DO_3 cell corresponding to β_1 phase can be constructed by joining $2 \times 2 \times 2$ B2 cells. Therefore, the lattice parameters of γ_2 and β_1 phases correspond approximately to three and two times that of B2, respectively, which results in extra (order) peaks in X-ray diffraction measurements that allow their identification. Finally, the α phase corresponds to the solid solution of Cu with Al.

It is the aim of this work to study the kinetics of the formation of γ_2 precipitates—and therefore the stability of

M. T. Ochoa-Lara · H. Flores-Zúñiga (✉) · D. Rios-Jara
Centro de Investigación en Materiales Avanzados, CIMAV, Miguel de Cervantes 120, Complejo Industrial Chihuahua, 31109 Chihuahua, Chih., Mexico
e-mail: horacio.flores@cimav.edu.mx

D. Rios-Jara
Instituto de Investigaciones en Materiales, UNAM, Ciudad Universitaria, Apdo. Postal 70-360, 04510 Mexico D.F., Mexico

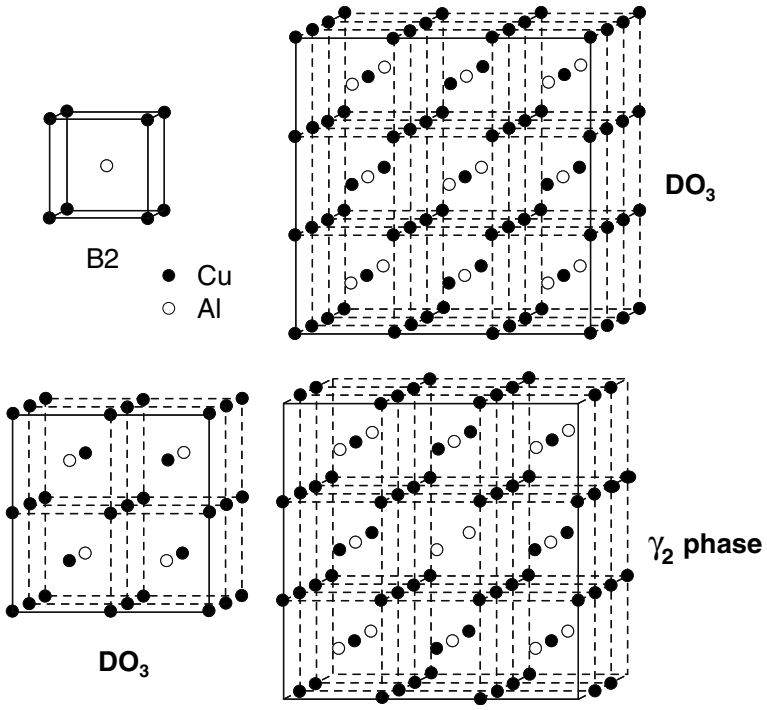

Fig. 1 B2 and DO_3 unit cells of the ordered β_1 phase and that of γ_2 phase. DO_3 can be constructed by eight B2 cells and the unit cell for γ_2 by 27 B2 unit cells, where vacancies are introduced at the center and corners of the resulting cell

β_1—at different aging temperatures. These results are of clear interest for the use of these alloys on a commercial basis.

Experimental procedure and results

Optical microscopy observations

A polycrystalline sample with composition Cu–10.45 Al–0.47Be wt% (Cu–22Al–3Be at%) was prepared by melting high purity elements in a controlled atmosphere induction furnace to avoid oxidation. After homogenization the measured martensitic start temperature (M_s) was set to –26 °C.

Samples of $5 \times 3 \times 3$ mm^3 were cut from the polycrystal. All samples were water quenched after a heat treatment of 15 min at 700 °C to obtain the metastable (DO_3 type ordered) β_1 phase at room temperature. In order to induce the formation of γ_2 precipitates, each specimen was submitted to different aging temperatures between 250 and 500 °C. Figure 2 shows a schematic of the performed heat treatments and Table 1 specifies the applied aging treatments. The samples were chemically etched for optical observation in 95 ml of ethanol, 2 grams of $FeCl_3$ and 2 ml of HCl solution.

The samples were observed in an optical microscope (Fig. 3). Precipitate mean size was measured using an image analyzer and the results are shown in Fig. 4.

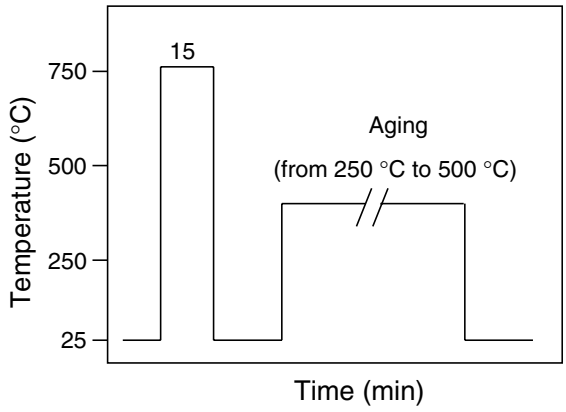

Fig. 2 Heat treatment applied to the samples

TEM observations

Disc shaped samples 3 mm in diameter and 120 μm in thickness were cut from the polycrystal. The same heat treatments showed in Fig. 2 were applied to the samples. The specimens for TEM were prepared by electropolishing using a solution of 25% H_3PO_4, 25% methanol and 50% water at –20 °C. Figure 5 compares TEM micrographs obtained at different temperatures and aging times. It is clear from these micrographs and also from those from optical microscopy that aging up to 250–300 °C for less than about 100 h keeps the amount of γ_2 precipitates on a reasonable level in order to expect a good behavior of the

Table 1 Thermal aging treatments

Temperature (°C) ± 3°C	Time (h)					
250	100	250	500	1500	2000	
300	100	200	400	800		
350	10	25	50	100	400	
400	1	3	5	10	15	24
500	1	3	5	10		

alloy concerning the previously mentioned thermomechanical properties.

XRD study

Ribbons of the alloy were preferred for X-ray studies, since a more convenient geometry is assured. Indeed, the flatness and small thickness of the Cu–Al–Be ribbons (~100 microns) produced by the melt spinning method assure that the sample is on the right plane for X-ray measurements. Composition and M_S for the samples are given in Table 2.

From each ribbon, 4 samples of $1 \times 0.5 \times 0.013$ cm were cut. All samples were quenched in water after maintaining a constant temperature of 700 °C for 15 min to form A2 phase. Each specimen was aged in an oven with controlled atmosphere at temperatures between 300 and 500 °C, in order to grow γ_2. Table 3 shows the aging

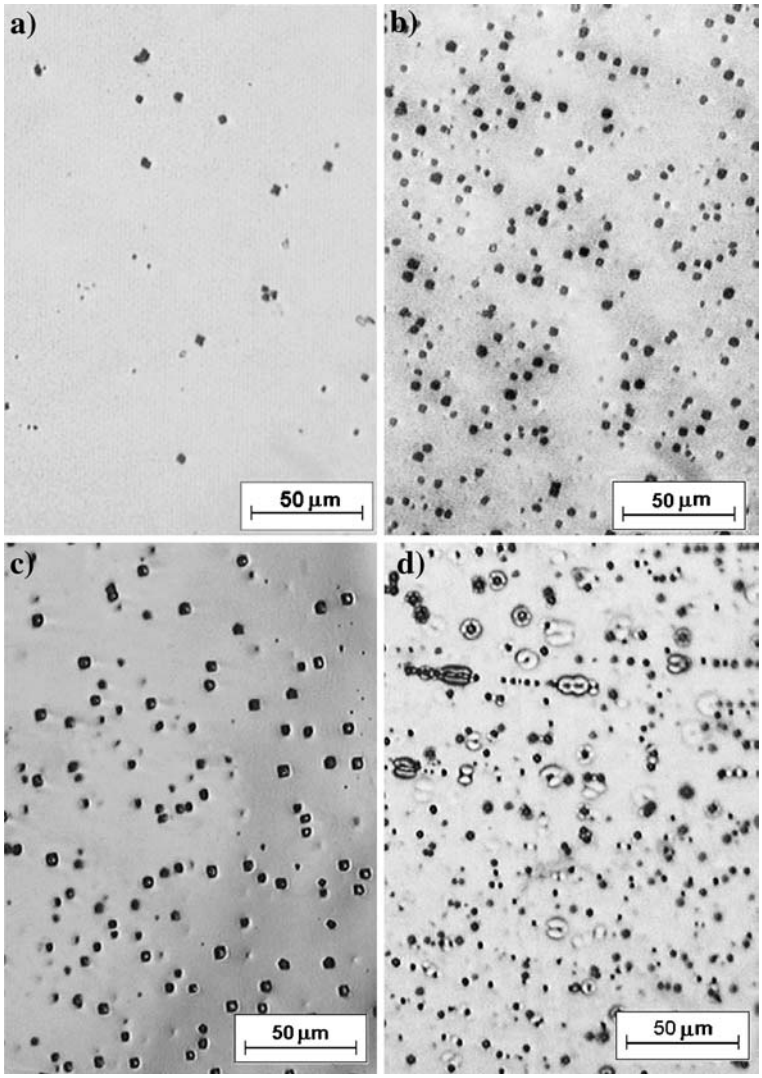

Fig. 3 Optical Micrographs of precipitates for different aging treatments: (**a**) 100 h at 300 °C, (**b**) 800 h at 300 °C, (**c**) 5 h at 500 °C, (**d**) 10 h at 500 °C

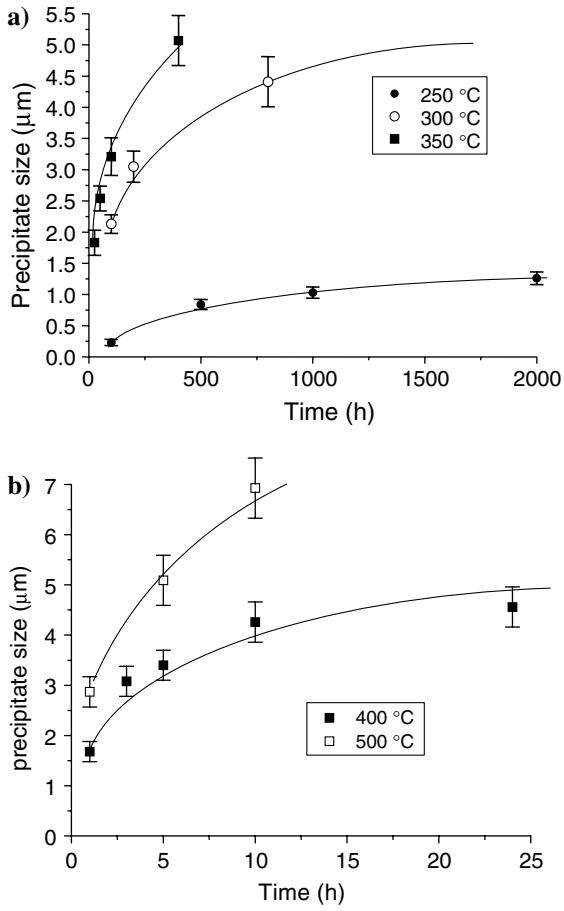

Fig. 4 Precipitates size evolution with time

treatments applied to each ribbon. Each sample was stuck to the θ–θ diffractometer holder with Ag paint and diffractograms were obtained at room temperature.

Table 2 Weight composition and transition temperature M_s for ribbons

Ribbon	Composition (% weight)	M_s(±2 °C)
C1	Cu–12.02%Al–0.445%Be	–63
C2	Cu–11.66%Al–0.437%Be	–60
C3	Cu–12.06%Al–0.447Be	–65
C4	Cu–12.05%Al–0.430%Be	–63

Table 3 Aging treatments

Temperature (±3 °C)	Aging time (h)			
300	264	456	600	840
350	192	336		
400	30	50	120(*)(**)	240(*)
500	20	30(*)	40(*)	

(*) Except C4

(**) Except C2

XRD measurements showed the evolution of γ_2 phase precipitates at the different aging temperatures (Fig. 6). Growth was observed through evolution of (211), (410) and (322) γ_2 peaks and the corresponding decrease in intensity of (111) and (200) DO_3 peaks. Note that at temperatures above 400 °C the (222) γ_2 peak appears as well.

Since the phase diagram of the alloy is well established, no differences in the kinetics of precipitation were expected from the X-ray studied ribbons and the corresponding bulk alloys. In fact, X-ray measurements (not presented here) were also performed in bulk samples with similar results and SEM observations of bulk samples confirmed the above conclusion, in agreement with other similar studies [3].

Discussion

Classical theory of diffusion

Data in Fig. 4a, b show a polynomial behavior with respect to time, of the kind $r = r_o + At^m$, where r is the ratio of the precipitate at time t, r_o is the initial ratio and m and A are constants. This behavior agrees with that proposed in the classical theory of diffusion-controlled growth by Wagner [8] and Lifshitz et al. [9]. Figure 7 shows the equivalent log–log graph of the data. Since no γ_2 precipitates were observed after quenching in all cases, r_o was set to cero. Therefore: $\log r = \log A + m \log t$.

Table 4 shows the values of the parameters measured in Fig. 7. From these results a mean value of $m = 0.33 \pm 0.03$ was obtained, which is in very good agreement with the $m = 1/3$ predicted by the classical theory. This result allows the conclusion that the different assumptions made

Table 4 Value of the constants in the polynomial adjustment

Temperature (±3 °C)	m (± 0.03)	A (μm/s$^{1/m}$)
250	0.34	0.2 ± 0.03
300	0.32	0.5 ± 0.05
350	0.29	0.8 ± 0.07
400	0.35	2. ± 0.2
500	0.34	3. ± 0.3

Table 5 Avrami's parameters

Temperature (±3 °C)	N	K (s^{-1})
250	0.68 ± 0.07	$4.0 \times 10^{-4} \pm 4 \times 10^{-5}$
300	0.76 ± 0.07	$1.0 \times 10^{-3} \pm 1 \times 10^{-4}$
350	0.82 ± 0.09	$1.0 \times 10^{-3} \pm 1 \times 10^{-4}$
400	0.94 ± 0.09	$3.0 \times 10^{-3} \pm 4 \times 10^{-4}$
500	1.1 ± 0.10	$1.0 \times 10^{-2} \pm 1 \times 10^{-3}$

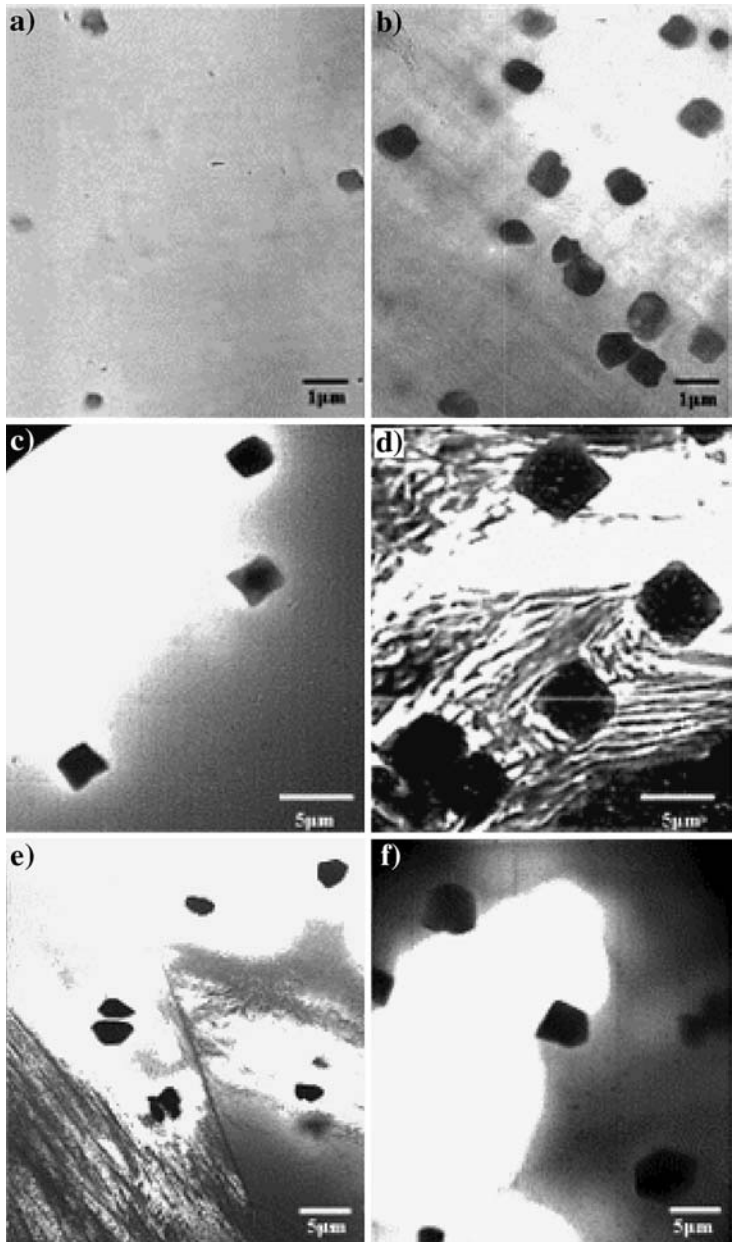

Fig. 5 Transmission electron micrographs of precipitates at different aging treatments: (**a**) 250 h at 250 °C, (**b**) 2000 h at 250 °C, (**c**) 25 h at 350 °C, (**d**) 400 h at 350 °C, (**e**) 10 h at 400 °C, (**f**) 24 h at 400 °C

by the classical theory regarding solubility, diffusion process, curvature ratio, etc., are valid for these alloys.

Avrami and TTT curves

In order to obtain a clearer idea of the kinetics of precipitation, the Avrami equation given by $y = 1–\exp(–kt^n)$ was considered. Here, y is the transformed fraction with the time t, k is a function of the transformation rate, and n is a constant that depends on the transformation mechanism. The transformed fraction was obtained by measuring the accumulated area of precipitates in a significant field of view from the optical images. Figure 8a shows the corresponding Avrami curves for different temperatures in $\log(\log(1/1–y))$ vs. $\log(t)$ representation, where experimental data superposed.

Table 5 shows k and n values for each curve. Constant k goes from 1.0×10^{-4} s^{-1} for 250 °C to 2×10^{-3} s^{-1} for 350 °C, and the mean value of n was 0.77, which is within the 0.5–2.5 range mentioned by Burke [10]. Additionally, TTT curves were constructed from this data and are presented in Fig. 8b.

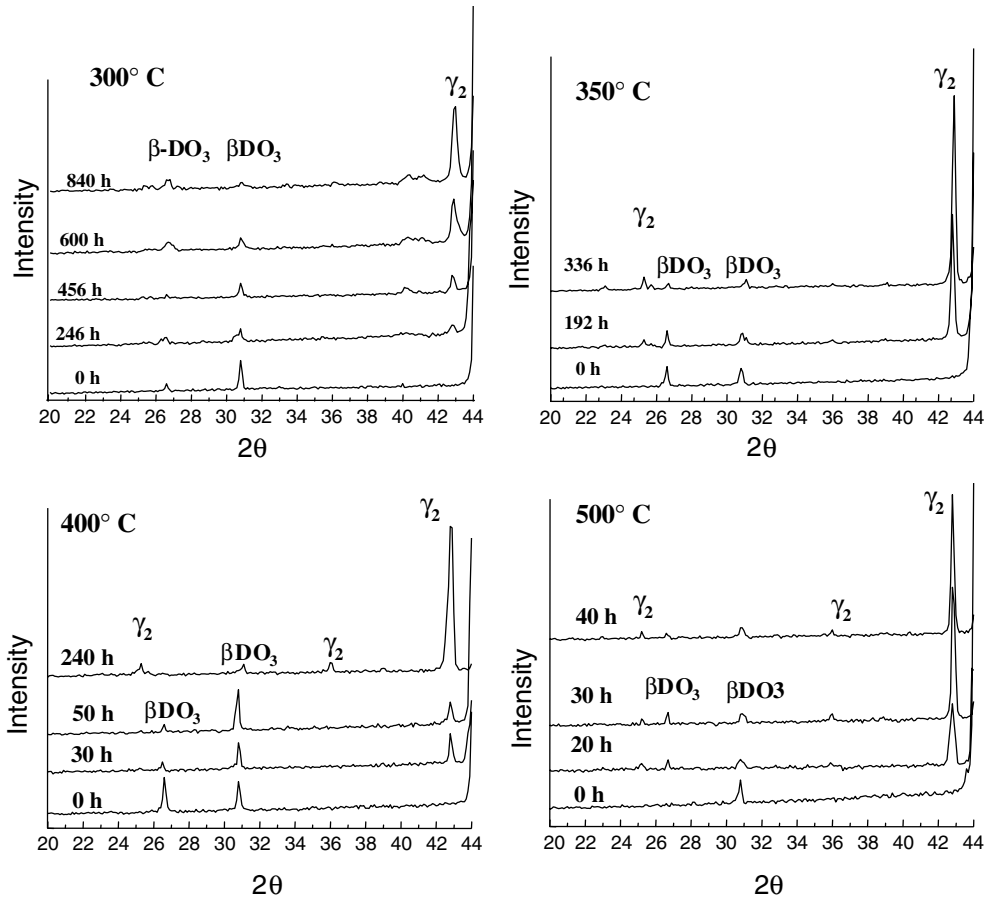

Fig. 6 X-ray diffractograms of Cu–Al–Be ribbons after aging at 300, 350, 400 and 500 °C for different times

The formation of α precipitates

Cu-rich α precipitates were also observed for the longer aging times at higher temperatures. Figure 9a, b show optical and SEM micrographs, where well-developed α regions surrounding former γ_2 precipitates are clearly visible. EDS measurements for the different zones are presented in Table 6where the directly measured mean composition values are considered, together with values corrected by taking into account the additional 3 at% Be in the polycrystalline sample and assuming Be atoms occupy Cu sites in the crystal structures of the three phases. With this correction, the measured values agree quite well (within less than 0.5%) with the expected values for all three phases.

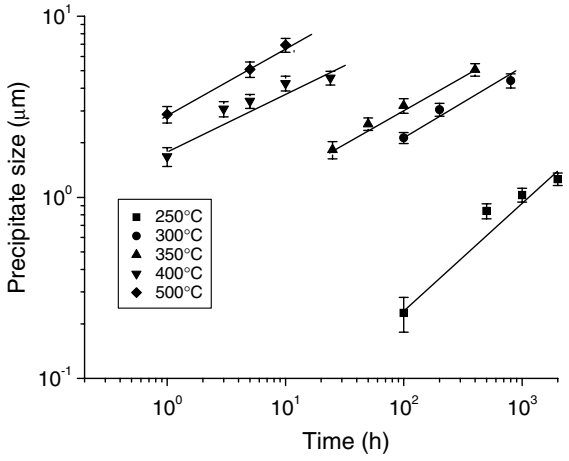

Fig. 7 Precipitate size as a function of time in logarithmic scale at different temperatures

The fact that γ_2 precipitates appear prior to those of α ones can be understood if one considers that the formation of the γ_2 crystal unit cell from 27 B2 unit cells (Fig. 1) may proceed through a mechanism of substitution of Cu atoms by vacancies; that is to say, no Al atoms must diffuse from β_1 for the Al content in the γ_2 cell to increase. Under these conditions what one should have first are γ_2 precipitates surrounded by Cu-rich β_1 regions. Since the interval of stability of β_1 extends to about 19 at% Al in the alloy (compared with the 22 at% Al of the original β_1 composition), this phase can accommodate an important amount of Cu atoms before it transforms to α phase. Therefore, α precipitates appear after γ_2 ones during the heat treatment

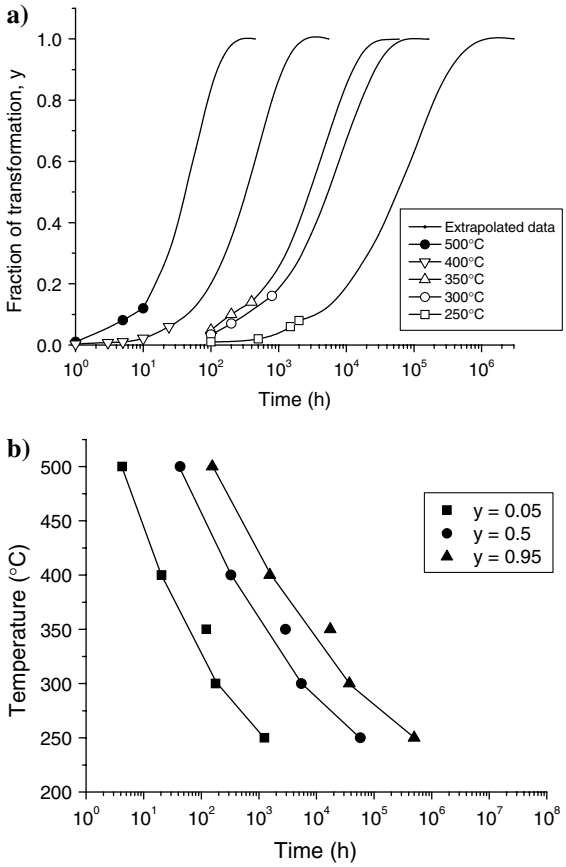

Fig. 8 (**a**)Avrami curves and (**b**) TTT curves obtained from results

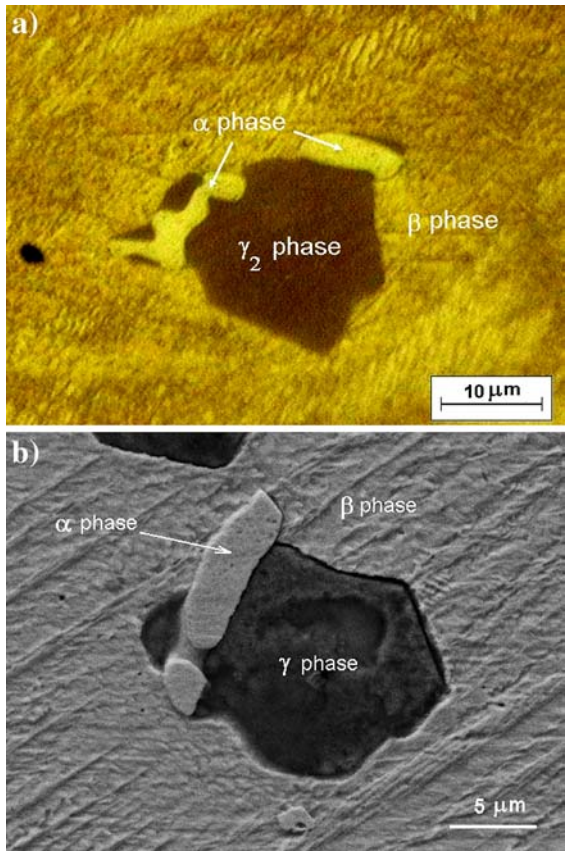

Fig. 9 (**a**) Optical photograph of the three different phases in a sample aged for 10 h at 500 °C. (**b**) SEM micrograph of a second region

and these were only observed after longer aging times at higher temperatures.

Conclusions

These results allow several conclusions regarding the high stability shown by the metastable β_1 phase of Cu–Al–Be alloys at temperatures suitable for many of the applications where shape memory alloys have been considered. Fitting the classical theory of diffusion-controlled growth quite well, the behavior of these alloys can be predicted, and new applications foreseen that are incompatible with other, older, Cu-based alloys.

Table 6 Chemical compositions of phases taken from EDS analysis in Fig. 9b

Phase	Direct measured values		Corrected values	
	Cu (at%)	Al (at%)	Cu (at%)	Al (at%)
Beta phase (Cu_3Al)	72.37	27.63	75.37	24.63
Gamma 2 phase (Cu_9Al_4)	66.15	33.85	69.15	30.85
Alfa phase (solubility limit 19.5 at% at 400°C)	77.23	22.77	80.23	19.77

Acknowledgements The authors wish to thank Armando Reyes for his invaluable help with X-ray characterizations. The authors also thank CONACYT—Mexico for the financial support given to this project.

References

1. Flores-Zúñiga H, Ríos-Jara D, Lovey FC, Guénin G (1995) J de physique IV.5:C2-171
2. Belkahla S, Flores-Zúñiga H, Guenin G (1993) Mater Sci Eng A169:119
3. Somoza A, Romero R (1999) J Appl Phys 85:130
4. Pons J, Cesari E (1999) Mater Str 6:115
5. Rapacioli R, Chandrasekaran M (1979) Proc Int Conf Martensitic Transformations. MIT Press, Cambridge, MA, USA, p 596
6. Cesari E, Pons J, Chandrasekaran M (1994) Trans Mat Res Soc Jpn 18:903
7. Lovey FC, Van Tendeloo G, Van Landuyt J, Chandrasekaran M, Amelinckx S (1984) Acta Metall 32:879
8. Wagner C (1961) Z Elektrochem 65:581
9. Lifshitz IM, Slyozov HI (1961) J Phys Chem Solids 19:35
10. Burke J (1965) The kinetics of phase transformations in metals, Pergamon Press, Oxford, p 240